Anomalous Broadening in Driven Dissipative Rydberg Systems

E. A. Goldschmidt,[1] T. Boulier,[2] R. C. Brown,[2,*] S. B. Koller,[2,†] J. T. Young,[2] A. V. Gorshkov,[2,3] S. L. Rolston,[2] and J. V. Porto[2,‡]

[1]United States Army Research Laboratory, Adelphi, Maryland 20783, USA

[2]Joint Quantum Institute, National Institute of Standards and Technology and the University of Maryland, Gaithersburg, Maryland 20899, USA

[3]Joint Center for Quantum Information and Computer Science, National Institute of Standards and Technology and the University of Maryland, College Park, Maryland 20742, USA

(Received 29 October 2015; published 16 March 2016)

We observe interaction-induced broadening of the two-photon $5s$-$18s$ transition in ^{87}Rb atoms trapped in a 3D optical lattice. The measured linewidth increases by nearly 2 orders of magnitude with increasing atomic density and excitation strength, with corresponding suppression of resonant scattering and enhancement of off-resonant scattering. We attribute the increased linewidth to resonant dipole-dipole interactions of $18s$ atoms with blackbody induced population in nearby np states. Over a range of initial atomic densities and excitation strengths, the transition width is described by a single function of the steady-state density of Rydberg atoms, and the observed resonant excitation rate corresponds to that of a two-level system with the measured, rather than natural, linewidth. The broadening mechanism observed here is likely to have negative implications for many proposals with coherently interacting Rydberg atoms.

DOI: 10.1103/PhysRevLett.116.113001

Because of their strong, long-range, coherently controllable interactions, Rydberg atoms have been proposed as a basis for quantum information processing and simulation of many-body physics [1–4]. Using the coherent dynamics of such highly excited atomic states, however, requires addressing challenges posed by the dense spectrum of Rydberg levels, the detrimental effects of spontaneous emission, and strong interactions. One approach is to operate on time scales much faster than the long Rydberg lifetime, typically microseconds to milliseconds [5–8]. Another proposed approach is to off-resonantly couple the ground and Rydberg state, admixing a small amount of the strongly interacting character into the ground state while substantially reducing spontaneous emission [9–19]. This Rydberg-dressed atom approach has been recently demonstrated with pairs of atoms [20], but has been difficult to realize in a many-body context [21]. A full understanding of the scope and limitations of these proposals requires including the effects of spontaneous decay within the dense energy level structure, which typically cannot be described by a mean-field treatment in interacting gases due to correlated quantum coherent and dissipative effects.

We study the effect of interactions in a driven, dissipative system of Rydberg atoms in a 3D optical lattice. We observe significant deviation from the expected excitation rates both on and off resonance that cannot be explained by van der Waals interactions or a mean-field treatment of the system. We attribute these effects to blackbody induced transitions to nearby Rydberg states of opposite parity, which have large, resonant dipole-dipole interactions with the state of interest. These off-diagonal exchange interactions result in complex many-body states of the system. Previous work has explored the impact of similar, controlled, interactions [22–25]; however, the uncontrolled creation of strongly interacting Rydberg levels due to spontaneous or blackbody processes is typically ignored in discussions of coherent Rydberg dynamics. These interactions may significantly modify the parameter regimes available for many-body Rydberg-based systems. In particular, we show that even at low densities of Rydberg atoms, uncontrolled production of atoms in other states significantly modifies the energy levels of the remaining atoms.

We use a state in ^{87}Rb with principal quantum number $n = 18$, and relatively short natural lifetime, $1/\Gamma_0 = 3.5\ \mu$s (including blackbody transitions), to study dissipative effects in a Rydberg system. Atoms in the same Rydberg level interact primarily via the C_6/r^6 van der Waals interaction, which for the $18s$ state is repulsive and equals the $18s$ linewidth at 800 nm separation. On the other hand, atoms in states of opposite parity interact via the much larger resonant dipole-dipole interaction, $\propto C_3/r^3$, whose angular dependence allows it to be positive or negative [26,27] and, for $18s$ interacting with $17p$ or $18p$, equals the $18s$ linewidth at 16 μm separation. Blackbody-induced transitions to other Rydberg levels constitute $\gtrsim$20% of the decay. We note that molecular resonances can be ignored due to the low principal quantum number that allows molecule formation only at extremely high densities [28].

We excite the $18s_{1/2}$ state using a two-photon transition via the $5p_{1/2}$ state [Fig. 1(a)], with intermediate state detuning $\Delta/2\pi \approx 235$ MHz and independently calibrated single-photon Rabi frequencies, $\Omega_1/2\pi < 10$ MHz and

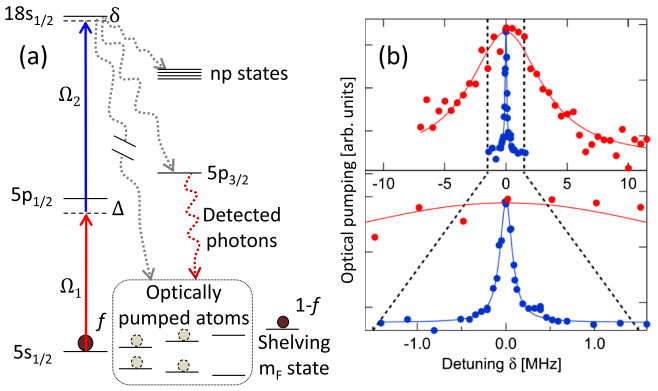

FIG. 1. (a) Level diagram for two-photon excitation to the $18s$ Rydberg level. Fractional density f in the $|F=2,m_F=-2\rangle$ ground state is controlled by microwave transfer, remaining atoms are shelved in the nonparticipating $|F=2,m_F=+2\rangle$ state (spectrally resolvable due to a 0.3 mT magnetic field along the optical axis). Decay from the $18s$ state occurs via many channels, including via Rydberg np levels and the $5p_{3/2}$ state. Atoms are optically pumped to the $|F=1,2;m_F=-1,0\rangle$ ground states. (b) Example $18s$ spectra measured as the population in the $m_F=0,\pm1$ states vs two-photon detuning δ. Blue is $\Omega/2\pi=3$ kHz, $f=0.3$ and red is $\Omega/2\pi=140$ kHz, $f=0.75$.

$\Omega_2/2\pi\approx 7$ MHz [29]. The two excitation lasers are stabilized to the same high-finesse optical cavity with <10 kHz linewidth, and are polarized and tuned to couple the ground $|5s_{1/2};F=2,m_F=-2\rangle$ hyperfine state to the $|18s_{1/2};F=2,m_F=-2\rangle$ state with two-photon detuning δ and Rabi frequency $\Omega=\Omega_1\Omega_2/2\Delta$.

The atomic system consists of a Bose-Einstein condensate of $\approx 4\times10^4$ atoms initially in the $|F=1,m_F=-1\rangle$ ground state, loaded into a 3D optical lattice [29,31]. The lattice provides a minimum separation of 406 nm and additionally suppresses superradiant Rayleigh scattering on the $5s$-$5p$ transition [32]. We control the atomic density available for Rydberg excitation with microwave rapid adiabatic passage that puts a fraction, f, of the atoms in the $|F=2,m_F=-2\rangle$ hyperfine state and shelves all remaining atoms in the nonparticipating $|F=2,m_F=+2\rangle$ state. This technique varies the average density $\rho_g=f\times 57\ \mu\text{m}^{-3}$ without altering the geometry of the cloud. We quantify excitation to the Rydberg state by measuring the population remaining in the initial state (or, equivalently, pumped into the initially empty $m_F=0,\ \pm1$ states) following excitation. The ground hyperfine populations are separated in time of flight with a Stern-Gerlach magnetic field gradient and measured via absorption imaging.

We measure the Rydberg excitation rate R (proportional to the optically pumped fraction following a fixed excitation time at least several $18s$ lifetimes, but shorter than the time to depump the initial state) as a function of δ, Ω, and ρ_g. Observed line shapes are symmetric and well characterized by Lorentzians [Fig. 1(b)]

$$R=\frac{R_0}{1+4\delta^2/\Gamma^2}. \quad (1)$$

We fit a decaying exponential to the population remaining in the initial state as a function of excitation time for two-photon excitation with $\delta=0$ and for the lower $5s$-$5p$ field alone [Fig. 2(a)]. For each Ω and ρ_g, we extract the resonant excitation rate R_0 by subtracting the $5s$-$5p$ optical pumping rate from the measured two-photon rate and scaling by the 45% fraction that decays to states other than the initial state. The linewidth Γ is determined from a Lorentzian fit to the optical pumping as a function of δ [Fig. 2(b)]. We observe that Γ increases dramatically with both Ω and ρ_g, reaching values as large as $\approx 200\Gamma_0$. At small Ω and ρ_g the narrowest observed linewidth is $\approx 3\Gamma_0$ and the residual broadening is attributed to inhomogeneities such as optical trapping light shifts and laser frequency noise.

Remarkably, R_0 is linear in Ω (with slope that depends on ρ_g) and shows no sign of saturation up to $\Omega=3\ \Gamma_0$ [Fig. 2(a)]. This behavior is inconsistent with standard single-atom theory and purely inhomogeneous broadening, which predicts faster excitation that depends on Ω^2 for

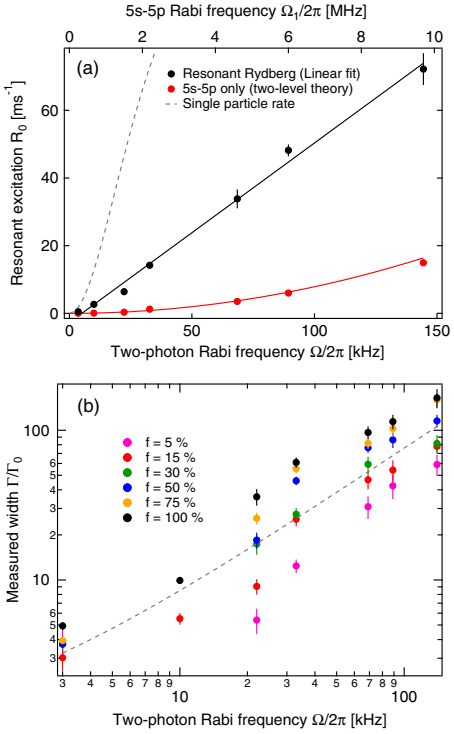

FIG. 2. (a) Measured optical pumping rate for $5s$-$5p$ field only (red) vs Ω_1 (top axis) and two-photon resonant excitation with lower rate subtracted (black) vs Ω (bottom axis). The black line is a linear fit to R_0 and the red line is the calculated $5s$-$5p$ rate with no adjustable parameters. The gray dashed line is the expected single particle rate. (b) Measured width Γ in units of the natural linewidth $\Gamma_0=2\pi\times 45$ kHz vs Ω for different fractional densities. The dashed line is linear scaling. Error bars represent statistical fitting uncertainties.

small Ω and saturates at large Ω [Fig. 2(a) dashed line]. The observed R_0 corresponds to a single-atom theory assuming the measured Γ as the transition linewidth: $R_0 \approx \Omega^2/\Gamma$.

To determine whether the observed broadening corresponds to a concomitant shortening of the $18s$ lifetime, as would broadening due to superradiance [33], we collect fluorescence emitted on the $5p_{3/2}$-$5s_{1/2}$ transition [Fig. 1(a)]. The fluorescence, which scales with the optical pumping signal and is proportional to the number of $18s$ atoms, is collected by a lens relay system (NA = 0.12) with an interference filter to block the $5s$-$5p_{1/2}$ excitation light, detected by a single photon avalanche diode, time tagged with 21-ns resolution, and summed over many excitation pulses. The observed lifetime, measured as the decay in detected photons after extinguishing the excitation light, is consistent with the 3.5 μs natural lifetime and independent of Ω (see Fig. 4 inset and Ref. [29] for more information). This result is consistent with previous observations of the suppression of superradiance due to driven dipole interactions [34]. The confirmation of the natural lifetime, along with the lack of saturation of the optical pumping, rules out superradiance and suggests the broadening is due to rapid dephasing of the optical coherence. In addition, confirmation of the lifetime allows an estimate of the steady-state $18s$ population.

The steady-state density of $18s$ atoms, under resonant excitation, is the atomic density ρ_g scaled by the ratio of the excitation rate R_0 to the decay rate Γ_0: $\rho_{18s} = \rho_g R_0/\Gamma_0$. The steady-state densities in nearby np states are equal to ρ_{18s} scaled by the ratios of the $18s$-np transition rates to the np decay rates: $\rho_{np} = \rho_{18s} b_{np}\Gamma_0/\Gamma_{np} = \rho_g R_0 b_{np}/\Gamma_{np}$, where b_{np} are the branching ratios from $18s$ to np (dominated by blackbody transitions to $17p$ and $18p$ states), and Γ_{np} are the decay rates of the np states (including blackbody transitions).

We observe Γ as large as 8 MHz, inconsistent with the 1.9 MHz van der Waals shift expected at our highest $18s$ densities [29]. In addition, the observed line shapes are symmetric, inconsistent with the repulsive van der Waals interaction. Also, the broadening depends only on the average density ρ_g and is independent of the microscopic configuration, which we alter by transferring atoms in every other lattice site in 2D to the shelving state [35]. The width, line shape symmetry, and insensitivity to nearest-neighbor spacing are consistent with the larger, longer-range, symmetric, dipole-dipole interaction between states of opposite parity.

For broadening due to dipole interactions, we expect a width of order $\sum |C_3^{(np)}|\rho_{np}$, where the sum is over the np states, which have different effective interaction strengths and branching ratios. This can be rewritten as $\beta_3\rho_g R_0$ using the expression above for ρ_{np} and defining the quantity $\beta_3 = \sum |C_3^{(np)}| b_{np}/\Gamma_{np} = 116\ \mu\text{m}^3$ (including the root-mean-squared average of the angular dependence of C_3). Combined with the observed relation $R_0 \approx \Omega^2/\Gamma$, this provides expressions for Γ and R_0 in terms of independently controlled variables Ω and ρ_g:

$$\Gamma \approx \Omega\sqrt{\rho_g\beta_3},$$
$$R_0 \approx \frac{\Omega}{\sqrt{\rho_g\beta_3}}. \quad (2)$$

Γ and R_0 are plotted in terms of these expressions in Fig. 3. The data not only collapse to approximately linear curves over 2 orders of magnitude, but the magnitude is well described by the dipole-dipole energy scale characterized by the independently calculated factor β_3. (Neither of these features is present for scaling with the van der Waals interaction [29]). This agreement is highly suggestive of a broadening mechanism dominated by dipole interactions with contaminant states. The fluctuating microscopic configuration of np states being populated and decaying leads to dephasing that is not accompanied by either saturated optical pumping or shortening of the lifetime.

This broadening mechanism requires some initial time to populate the contaminant states. We study the time dynamics of resonant and detuned excitation using the fluorescence on the $5p_{3/2}$-$5s_{1/2}$ transition. Figure 4 shows the fluorescence, converted into a number of $18s$ atoms, as a function of time for excitation at different detunings with $\Omega/2\pi = 140$ kHz and $f = 1$. At the two nonzero

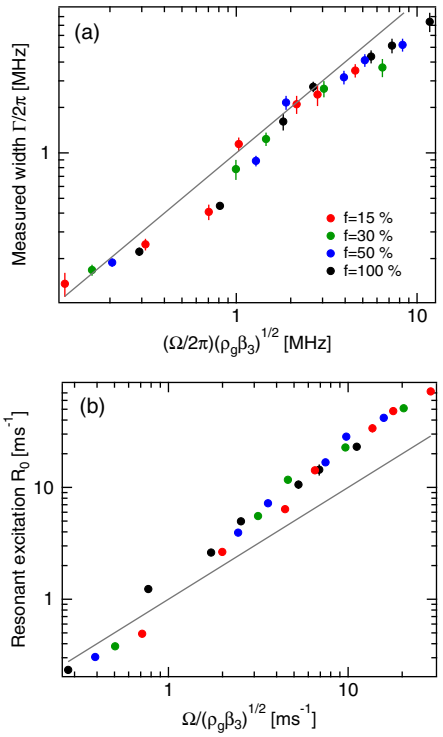

FIG. 3. (a) Measured width Γ vs $\Omega\sqrt{\rho_g\beta_3}$ and (b) resonant excitation rate R_0 vs $\Omega/\sqrt{\rho_g\beta_3}$ at different two-photon Rabi frequencies and densities. Linear scalings with unit slope are indicated with solid lines. Error bars represent statistical fitting uncertainties.

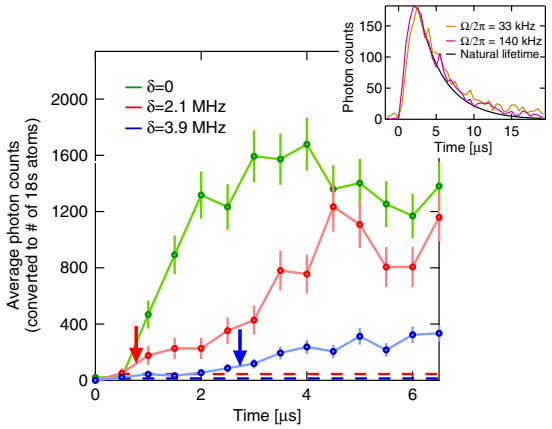

FIG. 4. Average fluorescence photon counts (converted to number of $18s$ atoms) as the excitation turns on for different two-photon detunings δ for $\Omega/2\pi = 140$ kHz and $f = 1$. Dashed lines indicate the number of excited atoms expected for the noninteracting, single particle scattering rates at those detunings. Arrows indicate the expected times to create the first contaminant atom for the detuned cases (see text). Error bars represent shot noise. Inset: Decay following short (2 μs) pulses for different two-photon Rabi frequencies with natural lifetime plotted for reference. All regimes are consistent with the $18s$ natural lifetime.

detunings, the population reaches a significant fraction of the resonantly excited population in a few μs. This is in stark contrast to the expected single-atom scattering times of 3 and 11 ms for these nominally far detuned cases ($\tau_s = 4\delta^2/\Gamma_0\Omega^2$ for $\delta \gg \Omega, \Gamma_0$). The faster excitation off resonance leads to observed $18s$ populations larger by a factor of $\gtrsim$30 than expected. For the resonant case, on the other hand, the observed population is smaller than expected from a single-atom picture by a factor of $\gtrsim$10, which cannot be explained by van der Waals interactions alone. The expected noninteracting excitation rates, both on and off resonance, are central to the feasibility of both dressed Rydberg proposals and Rydberg quantum gate implementations. We observe substantial deviations from these expected rates, which must be addressed for a full analysis of any Rydberg system.

This shortening of the off-resonant scattering time may not be a problem in few atom systems such as arrays of microtraps or other 2D systems [20,36,37], but it is likely problematic for implementing Rydberg-dressed atom proposals in large, many-body systems [9–12]. The time until the creation of the first contaminant atom is $\tau = \tau_s/bN_0$, where $b \gtrsim 20\%$ is the branching to contaminant states and N_0 is the total number of atoms. Interaction with the first np atom allows excitation of other atoms at a faster, resonant rate, leading to additional np atoms that, in turn, increase the number of atoms resonantly excited, similar to Rydberg aggregation at shorter time scales due to van der Waals shifts [38–40]. The long-range nature of the dipole interaction causes aggregation on length scales comparable to typical experimental system sizes, leading to rapid broadening over the entire ensemble. This simple time scale estimate gives a qualitative understanding of the early time dynamics, and future work to develop a full microscopic model will hopefully provide quantitative descriptions of both the dynamic and steady-state behavior [29]. Finally, the magnitude of the uncontrolled interactions with contaminant atoms is large compared to the interactions in a Rydberg-dressed approach. In particular, a dressed atom's uncontrolled dipole interaction with a contaminant atom is larger than its interaction with another dressed atom for $\rho_{np} > \Omega^2/\delta C_3$ [21], which is quickly exceeded under reasonable experimental conditions [29].

In conclusion, we report experimental observation of large spectral broadening of a Rydberg transition modifying the scattering rate both on and off resonance. We infer this effect results from the uncontrolled buildup of atoms in nearby Rydberg states. Resonant dipole-dipole interaction with those states causes dephasing and broadens the driven transition. Any single-atom approach to this problem is inherently nonlinear, as the broadening depends on the excited population, leading to distinctly non-Lorentzian line shapes that contradict our observations. Mean-field approaches fail because the off-diagonal interaction requires single-atom coherences between the driven state and contaminant states, which do not develop under blackbody induced population of the contaminant states [29]. This suggests the importance of correlations and is the focus of future theoretical efforts. Nonetheless, independent of a microscopic model, a simple analysis supported by experimental observation suggests the time available for coherent manipulations is much shorter than the expected single-atom scattering time, placing significant constraints on Rydberg dressing proposals. Importantly, the mechanism described here scales unfavorably with principal quantum number [29] and implies the need to account for even a small number of impurity Rydberg atoms when considering interactions in dense gases. And, although we have focused on exciting to an s state with contaminant p states, this mechanism is similarly present for excitation to any Rydberg state, which will populate nearby states of opposite parity. We note similar broadening has been observed in Rydberg transitions in strontium [41].

The authors thank T. C. Killian, F. B. Dunning, A. Browaeys, M. Foss-Feig, A. Hu, R. M. Wilson, and Z. X. Gong for helpful discussions. This work was partially supported by NSF PIF, AFOSR, ARO, ARL-CDQI, and NSF PFC at JQI.

*Present address: National Institute of Standards and Technology, Boulder, CO 80305, USA.
†Present address: Physikalisch Technische Bundesanstalt, 38116 Braunschweig, Germany.
‡porto@umd.edu

[1] H. Weimer, M. Müller, I. Lesanovsky, P. Zoller, and H. P. Büchler, Nat. Phys. **6**, 382 (2010).
[2] T. E. Lee, H. Häffner, and M. C. Cross, Phys. Rev. Lett. **108**, 023602 (2012).
[3] T. Pohl, C. S. Adams, and H. R. Sadephpour, J. Phys. B **44**, 180201 (2011).
[4] M. Saffman, T. G. Walker, and K. Mølmer, Rev. Mod. Phys. **82**, 2313 (2010).
[5] R. Heidemann, U. Raitzsch, V. Bendkowsky, B. Butscher, R. Löw, L. Santos, and T. Pfau, Phys. Rev. Lett. **99**, 163601 (2007).
[6] D. Barredo, H. Labuhn, S. Ravets, T. Lahaye, A. Browaeys, and C. S. Adams, Phys. Rev. Lett. **114**, 113002 (2015).
[7] V. Bendkowsky, B. Butscher, J. Nipper, J. P. Shaffer, R. Löw, and T. Pfau, Nature (London) **458**, 1005 (2009).
[8] E. Urban, T. A. Johnson, T. Henage, L. Isenhower, D. Yavuz, T. Walker, and M. Saffman, Nat. Phys. **5**, 110 (2009).
[9] J. E. Johnson and S. L. Rolston, Phys. Rev. A **82**, 033412 (2010).
[10] N. Henkel, R. Nath, and T. Pohl, Phys. Rev. Lett. **104**, 195302 (2010).
[11] G. Pupillo, A. Micheli, M. Boninsegni, I. Lesanovsky, and P. Zoller, Phys. Rev. Lett. **104**, 223002 (2010).
[12] J. Honer, H. Weimer, T. Pfau, and H. P. Büchler, Phys. Rev. Lett. **105**, 160404 (2010).
[13] A. W. Glaetzle, R. Nath, B. Zhao, G. Pupillo, and P. Zoller, Phys. Rev. A **86**, 043403 (2012).
[14] R. M. W. van Bijnen and T. Pohl, Phys. Rev. Lett. **114**, 243002 (2015).
[15] A. W. Glaetzle, M. Dalmonte, R. Nath, C. Gross, I. Bloch, and P. Zoller, Phys. Rev. Lett. **114**, 173002 (2015).
[16] I. Bouchoule and K. Mølmer, Phys. Rev. A **65**, 041803 (2002).
[17] T. E. Lee, S. Gopalakrishnan, and M. D. Lukin, Phys. Rev. Lett. **110**, 257204 (2013).
[18] A. Dauphin, M. Müller, and M. A. Martin-Delgado, Phys. Rev. A **86**, 053618 (2012).
[19] A. W. Glaetzle, M. Dalmonte, R. Nath, I. Rousochatzakis, R. Moessner, and P. Zoller, Phys. Rev. X **4**, 041037 (2014).
[20] Y.-Y. Jau, A. M. Hankin, T. Keating, I. H. Deutsch, and G. W. Biedermann, Nat. Phys. **12**, 71 (2016).
[21] J. B. Balewski, A. T. Krupp, A. Gaj, S. Hofferberth, R. Löw, and T. Pfau, New J. Phys. **16**, 063012 (2014).
[22] W. R. Anderson, J. R. Veale, and T. F. Gallagher, Phys. Rev. Lett. **80**, 249 (1998).
[23] H. Park, P. J. Tanner, B. J. Claessens, E. S. Shuman, and T. F. Gallagher, Phys. Rev. A **84**, 022704 (2011).
[24] G. Günter, H. Schempp, M. Robert-de-Saint-Vincent, V. Gavryusev, S. Helmrich, C. S. Hofmann, S. Whitlock, and M. Weidemüller, Science **342**, 954 (2013).
[25] E. Brekke, J. O. Day, and T. G. Walker, Phys. Rev. A **86**, 033406 (2012).
[26] I. I. Beterov, I. I. Ryabtsev, D. B. Tretyakov, and V. M. Entin, Phys. Rev. A **79**, 052504 (2009).
[27] K. Afrousheh, P. Bohlouli-Zanjani, D. Vagale, A. Mugford, M. Fedorov, and J. D. D. Martin, Phys. Rev. Lett. **93**, 233001 (2004).
[28] A. Derevianko, P. Kómár, T. Topcu, R. M. Kroeze, and M. D. Lukin, Phys. Rev. A **92**, 063419 (2015).
[29] See Supplemental Material at http://link.aps.org/supplemental/10.1103/PhysRevLett.116.113001, which includes Ref. [30], for further details.
[30] W. Li, I. Mourachko, M. W. Noel, and T. F. Gallagher, Phys. Rev. A **67**, 052502 (2003).
[31] J. Sebby-Strabley, M. Anderlini, P. S. Jessen, and J. V. Porto, Phys. Rev. A **73**, 033605 (2006).
[32] S. Inouye, A. Chikkatur, D. Stamper-Kurn, J. Stenger, D. Pritchard, and W. Ketterle, Science **285**, 571 (1999).
[33] T. Wang, S. F. Yelin, R. Côté, E. E. Eyler, S. M. Farooqi, P. L. Gould, M. Koštrun, D. Tong, and D. Vrinceanu, Phys. Rev. A **75**, 033802 (2007).
[34] J. Pellegrino, R. Bourgain, S. Jennewein, Y. R. P. Sortais, A. Browaeys, S. D. Jenkins, and J. Ruostekoski, Phys. Rev. Lett. **113**, 133602 (2014).
[35] P. J. Lee, M. Anderlini, B. L. Brown, J. Sebby-Strabley, W. D. Phillips, and J. V. Porto, Phys. Rev. Lett. **99**, 020402 (2007).
[36] J. Zeiher, P. Schauß, S. Hild, T. Macrì, I. Bloch, and C. Gross, Phys. Rev. X **5**, 031015 (2015).
[37] T. Xia, M. Lichtman, K. Maller, A. W. Carr, M. J. Piotrowicz, L. Isenhower, and M. Saffman, Phys. Rev. Lett. **114**, 100503 (2015).
[38] H. Schempp, G. Günter, M. Robert-de-Saint-Vincent, C. S. Hofmann, D. Breyel, A. Komnik, D. W. Schönleber, M. Gärttner, J. Evers, S. Whitlock, and M. Weidemüller, Phys. Rev. Lett. **112**, 013002 (2014).
[39] A. Urvoy, F. Ripka, I. Lesanovsky, D. Booth, J. P. Shaffer, T. Pfau, and R. Löw, Phys. Rev. Lett. **114**, 203002 (2015).
[40] N. Malossi, M. M. Valado, S. Scotto, P. Huillery, P. Pillet, D. Ciampini, E. Arimondo, and O. Morsch, Phys. Rev. Lett. **113**, 023006 (2014).
[41] B. J. DeSalvo, J. A. Aman, C. Gaul, T. Pohl, S. Yoshida, J. Burgdörfer, K. R. A. Hazzard, F. B. Dunning, and T. C. Killian, Phys. Rev. A **93**, 022709 (2016).